# Geodesic turnpikes for robot motion planning

Yann de Mont-Marin, Martial Hebert, Jean Ponce

# Geodesic turnpikes for robot motion planning

Yann de Mont-Marin[1,2][0000−0002−5446−595X], Martial Hebert[3][0000−0003−4566−5930], and Jean Ponce[2,4][0009−0000−5449−7620]

[1] Inria Paris, France
[2] Departement d'Informatique de l'ENS (CNRS, PSL Research University), France
[3] School of Computer Science, Carnegie Mellon University, United States
[4] Courant Institue and Center for Data Science, New York University, United States

**Abstract.** Endowing the configuration space of a robot with an appropriate metric structure and characterizing and computing the corresponding geodesics are central issues in motion planning. As recently observed in [23], the geodesics of SE(2) equipped with the so called minimum swept-volume distance exhibit in practice a behavior akin to the *turnpike property* in optimal control, with transient phases separated by a longer steady state close to prototypical trajectories, the *turnpikes* [32]. This presentation gives a theoretical counterpoint to this empirical observation with a formal definition of geodesic turnpikes using vector fields on Finsler manifolds, a simple differential characterization of geodesics in the case where the manifold is a Lie group and the Finsler distance is left-invariant, and, in the case where the corresponding operator is also reversible, a conjecture characterizing the turnpikes by vector fields satisfying simple conditions in the corresponding Lie algebras. As a proof of concept, closed-form (resp. numerical) procedures for computing the vector fields predicted by this conjecture are given for SE(2) equipped with the left-invariant Riemannian (resp. minimum swept-volume) distance introduced in [35] (resp. [23]) for rectangular shapes. The solutions empirically match, in both cases, the observed turnpike behavior of the corresponding geodesics. In the minimum swept-volume distance case, using the turnpikes for initialization also yields an order of magnitude speedup in computing geodesics.

**Keywords:** Turnpikes · Geodesics · Motion planning · Control Theory and Optimization

## 1 Introduction

### 1.1 Context

The configuration space of a robot and the corresponding forward kinematics can be represented in many different ways, notably in terms of the associated Lie group and Lie algebra [7]. The choice of the distance function used to endow this space with a metric structure, as well as the nature of the corresponding geodesics – roughly speaking, the locally or globally shortest paths in that space– play a key role in planning the best possible motions in tasks such as grasping,

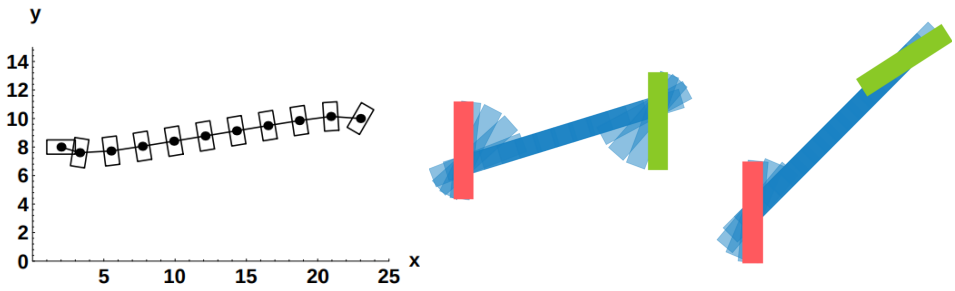


**Fig. 1.** Geodesics on SE(2) for a rotating and translating rectangle under **(left)** [35, Fig. 3(c)] a left-invariant Riemannian distance proposed in [35] and **(right)** the minimum swept-volume distance proposed in [23]. In both cases, the behavior of geodesics hints at a turnpike phenomenon. Reprinted with permission from [23, 35]. Copyright © 1998, 2023, IEEE.

manipulation and navigation in the presence of obstacles [19, 21, 26]. Conversely, this choice may be guided by various task heuristics, such as minimizing the chance of collision along a path [23, 25] or achieving some desired end-effector behavior [29].

Riemannian geometry and its Finslerian generalization provide a natural framework for constructing well-defined distances satisfying these heuristics and characterizing their geodesics. For example, Jaquier *et al.* [13, 14, 17] propose Riemannian geometry as a unifying framework for robot motion learning and control, and Ratliff *et al.* [28, 29, 33] use Finsler geometry to model motion policies called "geometric fabrics". The construction of geodesics is computationally challenging; thus, simple metric structures, for which closed forms are available, are commonly employed today despite their limited capacity for integrating heuristics. To go further, we need to leverage whatever favorable properties of specific distance are available to accelerate the computation of geodesics.

Figure 1 shows the geodesics joining two configurations of a rectangle rotating and translating in the plane associated with two distances over SE(2), a Riemannian distance introduced in Žefran *et al.* [35] (Fig. 1, left), and, the Finslerian minimum swept-volume distance proposed in de Mont-Marin *et al.* [23] (Fig. 1, right). In both cases, the motion along the trajectory is essentially, except near its endpoints, a pure translation parallel to the short side of the rectangle in the Riemannian case and to its long side in the Finslerian one. This behavior, where geodesics appear to stay close to simpler prototypical trajectories, except for short transient phases, is reminiscent of the turnpike phenomenon in optimal control [22, 30, 32]. Indeed, it can be shown that, for certain optimal control problems with a sufficiently large time horizon, any optimal trajectory remains, for most of the time, close to a turnpike, that is, the optimal solution of an associated stationary optimal control problem [30, 32]. In this setting, optimal trajectories can be decomposed into three segments: converging exponentially fast from the start point to the turnpike, spending most of their time there, and finally converging exponentially fast to the endpoint. Trélat and Zuazua have

also shown in [11, 32] that turnpikes can be used to initialize optimal control problems and significantly accelerate their computation.

To the best of our knowledge, the apparent turnpike behavior in Fig. 1 has not been formalized yet for Riemannian and Finslerian distances in the literature, nor has it been exploited in the efficient computation of geodesics. We give in Section 2 the mathematical background for our presentation. Following a construction similar to the one used in the optimal control setting [30], we introduce in Section 3 a framework for characterizing *geodesic turnpikes* as vector fields such that geodesic derivative remain close to these fields. We also propose a new Lie algebra formulation of the geodesic equation for left-invariant Finsler distances on Lie groups associated with robotic configuration spaces and combine this formulation with classical tools from dynamical systems [18] to propose a conjecture on the conditions for a left-invariant vector field to be a geodesic turnpike for a left-invariant Finslerian distance. Assuming it is true, we exploit this conjecture in Section 4 to find the vector fields for the examples illustrated in Fig. 1, analytically for the Riemannian distance on SE(2) proposed in [35] (Fig. 1, left), and numerically for the minimum swept-volume distance proposed in [23] (Fig. 1, right). In both cases, the vector fields match the turnpike behavior observed. We then use the corresponding turnpikes to initialize a geodesic solver and observe an order of magnitude speed-up for the minimum swept-volume distance.

Our main contributions are (1) a formal definition of geodesic turnpikes on Finsler manifolds (2) a geodesic equation for left-invariant Finsler distances on Lie groups (3) a conjecture providing a sufficient condition for a left-invariant vector field to be a geodesic turnpike (4) examples supporting the conjecture validity by predicting the empirical turnpike behavior of geodesics observed for two robotic related distance functions and (5) a proof of concept for accelerating geodesic computation using turnpikes for initialization.

### 1.2 Related work

**Metric structures on configuration spaces** have been explored extensively. For instance, Zhang *et al.* study the maximum vertex distance [36], previously proposed by Lavalle [21]. de Mont-Marin *et al.* construct the minimum swept-volume distance that reduces collision probabilities along geodesics [23]; and Žefran *et al.* provide a comprehensive examination of Riemannian geometries on the configuration space of a solid [34, 35], establishing properties necessary for a geometric structure to adhere to fundamental principles of mechanics.

**Turnpikes** have a long-standing history in finite-dimensional optimal control within econometrics [22]. Trélat and Zuazua introduce exponential turnpikes [32], providing a strong bound on the proximity between a trajectory and its turnpike and Sakamoto and Zuazua reformulated essential turnpike properties using geometric and dynamical system tools in [30], significantly influencing our current work. Faulwasser *et al.* introduce the concept of a velocity turnpike in [8], characterizing the turnpike not as a constant position but as a constant velocity. However, this notion needs revision for characterizing the turnpike behavior of

geodesics for reasons related to the inherent invariance of the solutions discussed in Sec. 2. Finally, turnpikes in robotics are closely related to the trim primitives studied in [10].

## 2 Background

### 2.1 Metric spaces

Consider some metric space $(X, d)$ defined by a set $X$ and a distance function $d : X^2 \to \mathbb{R}^+$. Let $I = [a, b]$ denote some interval of the real line and, given some positive integer $N$, let $s_N(I)$ denote the set of all sequences $t = \{t_0, t_1, \ldots, t_N\}$ of size $N + 1$ such that $a = t_0 < t_1 < \ldots < t_N = b$. Given a continuous parametric curve $\gamma : I \to X$, we define its *length* $L(\gamma)$ as [3]

$$L(\gamma) = \sup_{N \in \mathbb{N}^*, t \in s_n(I)} \sum_{i=0}^{N-1} d(\gamma(t_{i+1}), \gamma(t_i)). \tag{1}$$

We say that $\gamma$ is a rectifiable parametric curve when $L(\gamma)$ is finite. Given a parametric curve $\gamma : I \to X$, some interval $J$ and a continuous and monotone map $\phi : I \to J$, $\gamma \circ \phi$ is called a *reparameterization* of $\gamma$. The image of a parametric curve is invariant under parameterization, that is, $\gamma(I) = (\gamma \circ \phi)(J) \subset X$, and the length of a curve $L(\gamma)$ is also invariant under parameterization, $L(\gamma) = L(\gamma \circ \phi)$. The set of all reparameterizations of a parametric curve forms an equivalence class, the associated *geometric curve*, with a well-defined length. We say that a parametric curve *represents* the corresponding geometric curve. We say that a rectifiable parametric curve $\gamma$ represents a *geodesic* when, for any $t < t'$ in $I$ we have

$$L(\gamma|_{[t,t']}) = d(\gamma(t), \gamma(t')). \tag{2}$$

A *geodesic* is a geometric curve for which length and distance coincide on every curve segment. A parametric curve $\gamma$ represents a *local geodesic* if, for any $t$ in $I$ there exists some $\epsilon > 0$ such that $\gamma|_{[t-\epsilon,t+\epsilon]}$ represents a geodesic. Every geodesic is a local geodesic. There exists a unique parametric curve $\gamma : [0, 1] \to X$ with *constant velocity* representing any geodesic, such that for every $t$ in $[0, 1]$ we have

$$L(\gamma|_{[0,t]}) = td(\gamma(0), \gamma(1)), \tag{3}$$

which provides a canonical representative of the geodesic. We say that $(X, d)$ is a geodesic space if any two points $x, y$ in $X$ can be joined by a geodesic. Let $C^0(x, y)$ denote the set of all continuous parametric curves joining $x$ and $y$; the so-called Hopf-Rinow theorem provides a simple characterization of geodesic spaces

**Theorem 1 (Hopf-Rinow theorem).** *Let $(X, d)$ denote a complete and locally compact metric space such that for any pair of points $x, y$, there exists a rectifiable curve joining those points. The inner distance $d_i$ defined by*

$$d_i(x, y) = \inf_{\gamma \in C^0(x,y)} L(\gamma), \tag{4}$$

*is well-defined and* $(X, d_i)$ *is a geodesic space and the lengths defined in* (1) *using* $d$ *or* $d_i$ *are equal.*

The inner-distance construction (4) shows how to construct a geodesic space from a metric space satisfying certain assumptions. We assume from now on that $(X, d)$ is a geodesic space with $d_i = d$ since the configuration space distances used in robotics usually satisfy the hypotheses of Theorem 1.

If, in addition, $X$ is a $C^1$ manifold and $d$ is $C^1$, for any $C^1$ parametric curve $\gamma : [0, 1] \to X$ the quantity

$$\lim_{\epsilon \to 0^+} \frac{1}{\epsilon} d(\gamma(0), \gamma(\epsilon)) = \lim_{\epsilon \to 0^+} \frac{1}{\epsilon} L\left(\gamma|_{[0,\epsilon]}\right), \tag{5}$$

depends only on $x = \gamma(0)$ and $v = \dot{\gamma}(0)$, and we denote this quantity by $F(x, v)$ and say that $(F, X)$ is a Finsler manifold. We refer the reader to Bucataru [4] for an extended introduction to Finsler geometry. For any $x$ in $X$, the map $v \in T_x X \to F(x, v)$ is a norm on $T_x X$ [4] the tangent to $X$ in $x$ and $F(x, v)$ can be interpreted as the velocity of a curve passing in $x$ with derivative $v$. In particular, a parametric curve $\gamma : [0, 1] \to X$ has *constant velocity* if there exists a scalar $C > 0$ such that for all $t$ in $[0, 1]$, $F(\gamma(t), \dot{\gamma}(t)) = C$.

### 2.2 Finsler geodesics

For simplicity, let us assume from now on that $(X, F)$ is a $C^\infty$ Finsler manifold of dimension $n$ with associated distance $d$. As shown in [4] the length of a parametric curve $\gamma$ defined on $[0, 1]$ with endpoints, $x_0 = \gamma(0)$ and $x_1 = \gamma(1)$ verifies

$$L(\gamma) = \int_0^1 F(\gamma(t), \dot{\gamma}(t)) dt. \tag{6}$$

It is also convenient to define the *energy* function associated with the parametric curve $\gamma$ as

$$E(\gamma) = \frac{1}{2} \int_0^1 F^2(\gamma(t), \dot{\gamma}(t)) dt. \tag{7}$$

For completeness of our presentation, we present some properties proven in [4].

**Property 1.** *The global (resp. local) minimizers of* $L$ *among all parametric curves joining* $x_0$ *to* $x_1$ *represent geodesics (resp. local geodesics) joining these two points.*

**Property 2.** *The global (resp. local) minimizers of* $E$ *among all parametric curves joining* $x_0$ *to* $x_1$ *represent the local geodesics (resp. geodesics) between these two points with* constant velocity*. A geodesic joining* $x_0$ *to* $x_1$ *has one and only one representative that is also a minimizer of* $E$*. The minimizers of* $E$ *are canonical representatives for the geodesics joining* $x_0$ *to* $x_1$*. A minimizer of* $E$ *is also a minimizer of* $L$*, and the converse is true if and only if the parametric curve has constant velocity.*

A minimizer $\gamma^*$ of $E$ joining $x_0$ to $x_1$ is also a minimizer of $L$ and has constant velocity. Thus, there exists $C$ such that $F(\gamma^*(t), \dot{\gamma}^*(t)) = C$ for any $t$ in $[0,1]$. Substituting $C$ in both (6) and (7) yields

$$2E(\gamma^*) = L(\gamma^*)^2 = d(x_0, x_1)^2. \tag{8}$$

In addition, with the reparametrization $\phi : [0, d(x_0,x_1)] \to [0,1]$ such that $\phi(t) = \frac{t}{d(x_0,x_1)}$, we denote by $\gamma^\dagger = \gamma^* \circ \phi$, defined on $[0, d(x_0,x_1)]$, the unique parametrization of the geodesic with constant velocity 1, for all $t$ in $[0, d(x_0,x_1)]$ we have

$$F\left(\gamma^\dagger(t), \dot{\gamma}^\dagger(t)\right) = 1, \tag{9}$$

and we say that $\gamma^\dagger$ is parametrized by arclength. In the rest of the paper, $\gamma^*$ is always defined on $[0,1]$ and is a minimizer of the energy $E$, and $\gamma^\dagger$ is always the reparametrization by arclength of $\gamma^*$. Using the minimizers of $E$ provides a unique representation of the geodesics. Perhaps more importantly, $E$ can be used to characterize the geodesics by a differential equation. For this purpose, we introduce the fundamental bilinear form associated with the Finsler operator $F$. For any $(x,v)$ in $TX$ we define the bilinear form $g(x,v)$ on $T_xX$ by

$$g(x,v)(a,b) = \frac{1}{2}\,\frac{\partial^2}{\partial s \partial t} F^2(x, v + sa + tb)\Big|_{s=0,t=0}, \tag{10}$$

for any $a$ and $b$ in $T_xX$. Using the Euler-Lagrange equation from the calculus of variation, we obtain a new characterization of the geodesics.

**Property 3 (Geodesic equation).** *A necessary and sufficient condition for a $C^\infty$ parametric curve $\gamma$ to have constant velocity and represent a local geodesic is that it be a solution of the geodesic equation written in local coordinates $(x^i)$ using Einsteinian notation for $i,j,k,l$ in $1..n$ as*

$$g_{il}\ddot{\gamma}^i + \frac{1}{2}\left(\frac{\partial g_{lj}}{\partial x^k} + \frac{\partial g_{lk}}{\partial x^j} - \frac{\partial g_{jk}}{\partial x^l}\right)\dot{\gamma}^j\dot{\gamma}^k = 0, \tag{11}$$

*where the dependency in $\gamma$ and $\dot{\gamma}$ of $g$ is left implicit for conciseness and $\dot{\gamma}^i, g_{il}$ are the coordinates of the velocity and the Finsler tensor in the local basis of $T_{\gamma(t)}X$ associated with the local coordinates $(x^i)$.*

A minimizer of $E$ $\gamma^* : [0,1] \to X$ joining $x_0$ to $x_1$ and its reparameterization by arclength $\gamma^\dagger : [0, d(x_0,x_1)] \to X$ represent the same geodesic and have constant velocity, hence are solutions of the geodesic equation.

The bilinear form $g$ is a cornerstone in the study of local geodesics, and it enjoys several properties inherited from the homogeneity of $F$. In particular, for $(x,v)$ in $TX$, we have:

- $F^2(x,v) = g(x,v)(v,v)$,
- for any $\lambda > 0$, $g(x, \lambda v) = g(x,v)$,
- for any $w$ in $T_xX$, $\frac{1}{2}\,\frac{\partial}{\partial s} F^2(x, v+sw)\big|_{s=0} = g(x,v)(v,w)$.

The first two results are given in [4], however for completeness of the paper, proofs of these results and others crucial for Proposition 2 in Sec. 3 are presented in Appendix A.

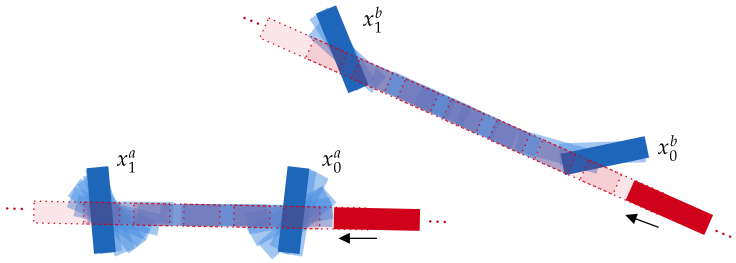


**Fig. 2.** Illustration of geodesic turnpikes. In blue, we plot two Finslerian geodesics of the minimum swept-volume distance [23], joining $x_0^a$ with $x_1^a$ and $x_0^b$ with $x_1^b$. In red, we plot integral curves of $V$, the vector field of instantaneous translations parallel to the long side of the rectangle. $V$ is supposedly a geodesic turnpike, as we observe that integral curves of $V$ approximate the geodesics well except at their start and end points.

## 3 Lie groups and geodesic turnpikes

### 3.1 Motivation for robotic applications

In robotics, the configuration space is often a Lie Group. For instance, the configuration space for a free-flying robot is SE(3) the group of rigid placements, and for a serial manipulator arm with six joints, it is $\mathrm{SO}(2)^6$. These spaces are typically equipped with a smooth Finsler operator. For example, SE(3) is generally equipped with the left-invariant canonical Riemannian distance [9] for which the geodesics can be obtained in closed form. However, for more complex distances, such as the minimum swept-volume distance in [23], the geodesics are not available in closed form and must be computed by solving the problem

$$\min_{\gamma \in \mathcal{C}^\infty([0,1],X)} \frac{1}{2} \int_0^1 F^2(\gamma(t), \dot{\gamma}(t)) dt, \quad \text{s.t.} \quad \gamma(0) = x_0 \quad \text{and} \quad \gamma(1) = x_1, \quad (12)$$

for any $x_0$ and $x_1$ in $X$.

This problem can be solved using off-the-shelf minimization software such as [12, 27] on a discretized version of (12), or with a bounded value ODE solver, such as [15], using the induced geodesic equation (11) and boundary conditions $\gamma(0) = x_0$ and $\gamma(1) = x_1$. In both cases, initialization has a crucial impact on the performance of the algorithms because the underlying minimization problems are not necessarily convex. The geodesics of [23, 35], illustrated in Fig. 1, suggest a turnpike behavior.

We propose formalizing this behavior in terms of *geodesic turnpikes* using vector fields. We can then initialize geodesic solvers efficiently using these vector fields, as presented in Section 4.

### 3.2 Geodesic turnpike definition

Let $(X, F)$ denote a Finsler manifold, and $d$ denote the associated distance. Let $V$ denote a smooth vector field on $X$. Qualitatively, $V$ is a geodesic turnpike for $F$ on $X$ if every parametrization $\gamma^\dagger$ by arclength of a geodesic has its derivative

$\dot{\gamma}^\dagger$ *"close"* to $V$. Figure 2 illustrates the idea in the case where $X = \mathrm{SE}(2)$, $F$ is the operator for the minimum swept-volume distance [23] and $V$ the vector field of instantaneous translations parallel to the long side of the rectangle, illustrated with a black arrow. We observe that for each geodesic, an integral curve of $V$ approximates the geodesic well except near its start and endpoints. To formalize the notion of *"close"*, we propose a definition of *exponential geodesic turnpike* inspired by exponential turnpikes in the context of optimal control [32].

**Definition 1 (Exponential geodesic turnpike).** *We say that a smooth vector field $V$ is an exponential geodesic turnpike for $F$ on $X$ if there exist constants $K > 0$ and $\sigma > 0$ such that for any $x_0, x_1$ in $X$, there exist $\alpha$ in $\{-1, 1\}$ such that $\gamma^\dagger : [0, d(x_0, x_1)] \to X$ the parametrization by arclength of a geodesic joining $x_0$ and $x_1$ verifies for all $t$ in $[0, d(x_0, x_1)]$*

$$F\left(\gamma^\dagger(t), \alpha\dot{\gamma}^\dagger(t) - V_{\gamma^\dagger(t)}\right) \leq K\left(e^{-\sigma t} + e^{-\sigma(d(x_0,x_1)-t)}\right). \tag{13}$$

If $\gamma^\dagger$ joins $x_0$ to $x_1$, its time-reversed reparameterization connects $x_1$ to $x_0$, and its derivative has the opposite sign. Using $\alpha$ in $\{-1, 1\}$, we can concisely state that any parameterization by arc length or its time-reversed reparameterization possesses an exponential bound around $V$. The left-hand side of Eq. (13) is the distance between $\dot{\gamma}^\dagger(t)$ and $V_{\gamma^\dagger(t)}$ because the mapping $v \mapsto F(x, v)$ is a norm on $T_x X$. The right-hand side of Eq. (13) is an exponential upper bound. The bound is loose for $t$ near 0 due to the first term and for $t$ near $d(x_0, x_1)$ due to the second term. The bound tightens exponentially when $t$ is far from the boundaries of $[0, d(x_0, x_1)]$. Figure 3 illustrates qualitatively this behavior for a minimum swept-volume distance geodesic [23]. In the proposed formalism, the turnpike is a vector field, and the bound is in the space of velocities. In this sense, it resembles the velocity turnpikes [8].

It is important to note that $K$ and $\sigma$ does not depend on $x_1$ and $x_2$, and thus the upper bound in Definition 1 do not depend on $x_1$ and $x_2$, but only on the distance $d(x_0, x_1)$ between those points. It implies that with a given precision, the length of the geodesic segment for which the velocity bound (13) is looser than $\epsilon$ does not depend on the total geodesic length.

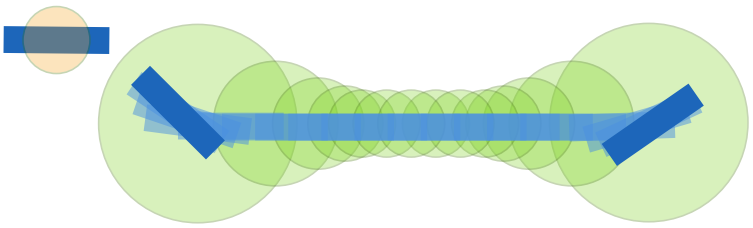

**Fig. 3.** Illustration of an exponential geodesic turnpike bound for a geodesic of the minimum swept-volume distance [23]. For visualization, an orange disc is rigidly attached to the blue rectangle. The exponential bound on the velocity in Definition 1 induces a maximum displacement of the orange disc during a time interval $\Delta t > 0$ around the geodesic turnpike $V$. For each time step, we represent, in green, the area that the orange disc can cover, given the maximum displacement. The union of these green discs provides an upper bound on the workspace region, as guaranteed by the exponential bound for the orange disc rigidly attached to the rectangle.

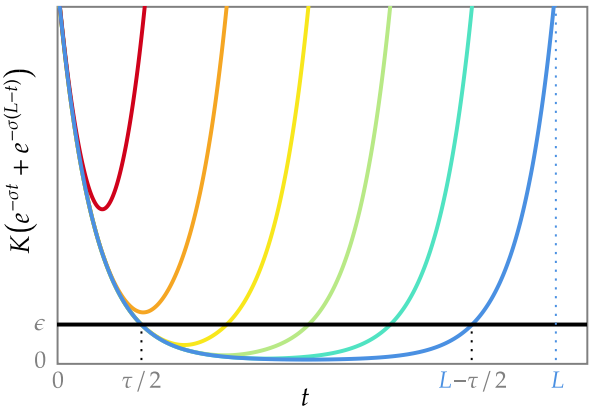


**Fig. 4.** To illustrate Proposition 1, we plot the right-hand side (13) as a function of the arclength $t$ of geodesics of various lengths $L$. Given an $\epsilon > 0$, there exists a $\tau > 0$ such that for any geodesic, the velocity is guaranteed to be upper-bounded by $\epsilon$ whenever $\tau/2 < t < L - \tau/2$. The first two curves (red and orange) correspond to geodesics with lengths lower than $\tau$.

**Proposition 1.** *For any $\epsilon > 0$, there exists $\tau > 0$ such that for any curve $\gamma^\dagger$ parametrized by arclength and representing a geodesic, if $I_\epsilon$ denote the set of $t$ such that $F\left(\gamma^\dagger(t), \dot{\gamma}^\dagger(t) - V_{\gamma^\dagger(t)}\right) \geq \epsilon$ we have*

$$L\left(\gamma^\dagger|_{I_\epsilon}\right) \leq \tau. \tag{14}$$

The proof is given in Appendix B and Fig. 4 illustrates this proposition. Proposition 1 ensures that integral curves of $V$ are a good approximation of "long" geodesics. This is because $\tau$ depends only on $\epsilon$ and not on any particular geodesic or its length $L$. As a result, $\tau/L \to 0$ as $L \to \infty$, meaning that the larger $L$ is, the better the approximation becomes. In the example of Fig. 1 (right), even configurations that appear "close" in the workspace have a "long" geodesic length from the point of view of the turnpike property.

Having defined geodesic turnpikes, we now examine the specific case typical in robotics, where $X$ is a Lie group and the operator $F$ demonstrates some invariance [8].

### 3.3 Left-invariant Finsler operators on Lie groups

We now study the case of invariant reversible Finsler distances on Lie groups to identify sufficient conditions for characterizing geodesic turnpikes. From now on, $X$ is a Lie group. Given some $h$ in $X$, we denote by $\tilde{L}_h$ the *left tangent action*, which describes how the tangent vectors at different points in the group are related through left multiplication (see Chirikjian [6] for further details on Lie groups). For any $x$ in $X$, $\tilde{L}_h : T_xX \to T_{h\circ x}X$ is a linear isomorphism. We say that $F$ is left-invariant on $X$, if for every $(x, v)$ in $TX$ and $h$ in $X$,

$$F(x, v) = F(h \circ x, \tilde{L}_h v), \tag{15}$$

i.e., the Finsler operator does not change when we compose $x$ on the left with a group element $h$ and apply the associated left tangent action on $v$. In particular,

with $h = x^{-1}$, we have $F(x, v) = F(e, \tilde{L}_{x^{-1}} v)$ where $e$ denote the identity element of $X$. Let $C(u) = \frac{1}{2}F^2(e, u)$ denote the cost function used in (12) restricted to the Lie algebra $\mathfrak{X}$ and let $u : [0, 1] \to \mathfrak{X}$ defined by $u(t) = \tilde{L}_{\gamma(t)^{-1}} \dot{\gamma}(t)$, then (12) is equivalent to

$$\begin{aligned} &\min_{\gamma \in \mathcal{C}^\infty([0,1],X), u \in \mathcal{C}^\infty([0,1],\mathfrak{X})} \int_0^1 C(u(t))dt, \\ &\text{s.t} \quad \forall t \in [0, 1], \quad \dot{\gamma}(t) = \tilde{L}_{\gamma(t)} u(t), \\ &\qquad \gamma(0) = x_0, \\ &\qquad \gamma(1) = x_1, \end{aligned} \tag{16}$$

because $\tilde{L}_{\gamma(t)^{-1}} = \tilde{L}^{-1}_{\gamma(t)}$. As shown in Appendix C, the calculus of variations can now be used to obtain a more tractable geodesic equation associated with (16) than the general one (11):

**Proposition 2.** *If $F$ is a left-invariant Finsler distance on the Lie group $X$, then the geodesic equation associated with* (16) *can be written in some basis of the Lie algebra $\mathfrak{X}$ as:*

$$\begin{aligned} \dot{\gamma}(t) &= \widetilde{L}_{\gamma(t)} u(t), \\ \dot{u}(t) &= G^{-1}_{u(t)} \operatorname{ad}^\top_{u(t)} G_{u(t)} u(t), \end{aligned} \tag{17}$$

*where $G_u$ denotes the matrix representation of $g(e, u)$ in the chosen basis,* $\operatorname{ad}_u$ *denotes the matrix representation in that basis of the Lie algebra adjoint operator* $\operatorname{ad}_u$*, which captures the action of $u$ on the rest of the algebra via the Lie bracket on $\mathfrak{X}$. The solutions represent local geodesics and do not depend on the choice of basis.*

In the Riemannian case, $G_u$ is independent of $u$, and we recover the so-called Euler-Arnol'd equation [2]. We feel that Proposition 2 should be textbook material since it resembles classical results [5, 20] but, to the best of our knowledge, this geodesic equation for invariant Finsler distances has not been written in this form yet.

### 3.4 Geodesic turnpikes for left-invariant Finsler distances

Let us now study the dynamics given by the geodesic equation (17) of the left-invariant Finsler operator $F$ on $X$. The objective is to construct a vector field $V$ that is an exponential geodesic turnpike for $F$ on $X$ as defined in Definition 1. Any parametric curve $\gamma^*$ solution of the minimization problem (16) is a solution of the geodesic equation (17). Its reparametrization $\gamma^\dagger$ by arclength, defined on $[0, L]$ and representing the same geodesic, is also a solution of the geodesic equation (17). In particular, $u(t) = \tilde{L}_{\gamma^\dagger(t)^{-1}} \dot{\gamma}^\dagger(t) = \tilde{L}^{-1}_{\gamma^\dagger(t)} \dot{\gamma}^\dagger(t)$ is a solution of $\dot{u} = D(u)$ where $D$ denote the dynamics function on the lie algebra $\mathfrak{X}$: $D(u) = G_u^{-1} \operatorname{ad}_u^\top G_u u$. The solutions of the geodesic equation have a constant velocity,

and $\gamma^\dagger(t)$ is parametrized by arclength, so we have for any $t$ in $[0, L]$, $F(e, u(t)) = F(\gamma^\dagger(t), \dot{\gamma}^\dagger(t)) = 1$. Thus, the dynamical system $\dot{u} = D(u)$ is well-defined on $\mathbb{S}_F(1)$, the unit sphere associated with $F$ and defined as the set of all $u$ in $\mathfrak{X}$ such that $F(e, u) = 1$. Therefore, we study the dynamics associated with $D$ on $\mathbb{S}_F(1)$. The lie algebra elements $\bar{u}$ of $\mathbb{S}_F(1)$ verifying $D(\bar{u}) = 0$ are the *equilibrium points* of the dynamics on $\mathbb{S}_F(1)$. Using the homogeneity properties of Finsler operators, we obtain the following characterization of these points:

**Proposition 3.** *An element $\bar{u}$ in the lie algebra $\mathfrak{X}$ is an equilibrium point of the dynamics $D$ on $\mathbb{S}_F(1)$ if and only if*

$$\mathrm{ad}_{\bar{u}}^\top G_{\bar{u}} \bar{u} = 0, \quad \bar{u}^\top G_{\bar{u}} \bar{u} = 1, \tag{18}$$

*In addition, the tangent space $T_{\bar{u}}\mathbb{S}_F(1)$ tangent to $\mathbb{S}_F(1)$ in $\bar{u}$ is the set of elements $v$ in $\mathfrak{X}$ such that $v^\top G_{\bar{u}} \bar{u} = 0$ and the Jacobian of the dynamics around $\bar{u}$ is*

$$J_{\bar{u}} = G_{\bar{u}}^{-1}(\mathrm{ad}_{\bar{u}}^\top G_{\bar{u}} + \mathrm{P}_{G_{\bar{u}}\bar{u}}), \tag{19}$$

*where $\mathrm{P}_{G_{\bar{u}}}$ is the unique matrix defined by*

$$\forall v \in \mathfrak{X}, \quad \mathrm{P}_{G_{\bar{u}}} v = \mathrm{ad}_v^\top G_{\bar{u}}. \tag{20}$$

Note that $\mathrm{P}_{G_{\bar{u}}}$ is well defined because the mapping $v \mapsto \mathrm{ad}_v$ is linear. The proof of the proposition can be found in Appendix D.

The dynamics around the equilibrium point are given by the spectrum of $J_{\bar{u}}$ [18]. As we study the dynamics on $\mathbb{S}_F(1)$, we restrict the Jacobian to the tangent space $A = T_{\bar{u}}\mathbb{S}_F(1)$. From [30], we know that exponential bounds typically occur around an equilibrium point when it is a saddle point.

**Definition 2 (Saddle point on the unit sphere).** *An equilibrium point $\bar{u}$ of the dynamics $D$ on $\mathbb{S}_F(1)$ is called a saddle point when all eigenvalues of the endomorphism $J_{\bar{u}}|_A$ have nonzero real parts, at least one of which has a positive real part, and at least another one has a negative real part.*

The theory of dynamical systems [18] gives a general characterization of saddle points. Sakamoto *et al.* [30] sum up many of those results, with particular attention to the existence of exponential bounds for a dynamical system around saddle points. In our setting, we say that a sub-manifold $M$ of $\mathbb{S}_F(1)$ is invariant if any solution of the dynamics $\dot{u} = D(u)$ with $u(0)$ in $M$ remains in $M$ for all time $t$. Let $\bar{u}$ denote a saddle point on the unit sphere $\mathbb{S}_F(1)$ of dimension $m = n - 1$. It is shown in [18] that there exists an invariant sub-manifold $S$ of $\mathbb{S}_F(1)$ of dimension $k$ tangent to the eigenvectors of $J_{\bar{u}}|_A$ associated with positive eigenvalues and called the *stable manifold* and an invariant sub-manifold $U$ of $\mathbb{S}_F(1)$ of dimension $m - k$ tangent to the eigenvectors of $J_{\bar{u}}|_A$ associated with negative eigenvalues and called the *unstable manifold*. Sakamoto *et al.* [30, Th. 3] prove the following theorem:

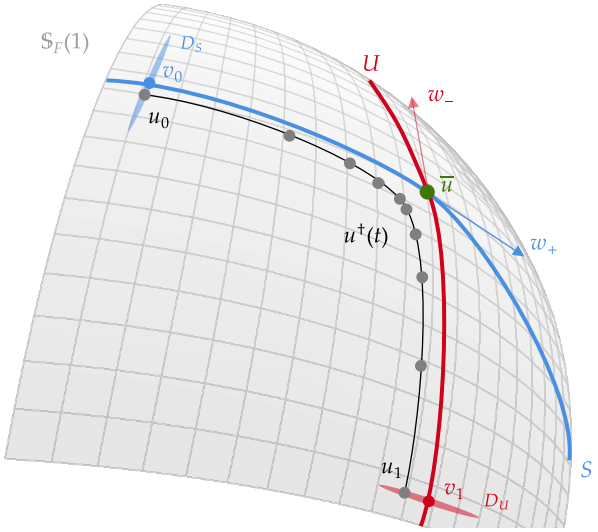


**Fig. 5.** Illustration of Theorem 2. We plot a portion of the surface $\mathbb{S}_F(1)$ around a saddle point $\bar{u}$ of the Lie algebra dynamics $\dot{u} = D(u)$. We show an eigenvector $w_+$ associated with a positive eigenvalue tangent to the stable manifold $S$ and, in red, an eigenvector $w_-$ associated with a negative eigenvalue tangent to the unstable manifold $U$. We plot the discs $D_S$ and $D_U$ transversal to $S$ in $u_0$ and to $U$ $u_1$. A solution $u^\dagger$ of the dynamics with $u^\dagger(0) = u_0$ in $D_S$ and $u^\dagger(L) = u_1$ in $D_U$ is shown in black, and it verifies the conditions of Theorem 2. The distance $\|u^\dagger(t) - \bar{u}\|$ is bounded exponentially. We draw the points $u^\dagger(t_i)$ as small gray discs for $i = 0..9$ where the sequence $t_i = iL/9$ forms a regular partition of $[0, L]$. The distribution of the samples $u^\dagger(t_i)$ illustrates the behavior induced by the exponential bound: $u^\dagger$ goes quickly toward the saddle point, slows down near it, and finishes fast toward the endpoint $u_1$.

**Theorem 2.** *Let $u \to ||u||$ be a norm on $\mathfrak{X}$. For any $v_0$ in $S$, any $v_1$ in $U$, any $(m-k)$-dimensional disc $D_S$ transversal to $S$ at $v_0$, and any $k$-dimensional disc $D_U$ transversal to $U$ at $v_1$, there exist constants $T > 0$, $K > 0$ and $\sigma > 0$ such that for every $L > T$, there exists $\rho > 0$, $u_0$ in $B(v_0, \rho) \cap D_S$ and $u_1$ in $B(v_1, \rho) \cap D_U$ such that there exists a solution $u^\dagger$ of the dynamics $D$ with $u^\dagger(0) = u_0$ and $u^\dagger(L) = u_1$ and for any $t$ in $[0, L]$*

$$\|u^\dagger(t) - \bar{u}\| \leq K \left( e^{-\sigma t} + e^{-\sigma(L-t)} \right). \tag{21}$$

*Moreover, $\rho \to 0$ when $L \to \infty$.*

This theorem is illustrated by Fig. 5. Informally around a saddle point, we have families of trajectories, indexed by choice of $v_0$, $v_1$, $D_S$, and $D_U$, with endpoints in $D_S$ and $D_U$ that can have arbitrarily long durations and spend most of their time very close to the saddle point. All elements of a family share the constant $T$, $K$, and $\sigma$.

Multiple technical subtleties prevent a straightforward use of the theorem in the geodesic problem case. First, we do not have any conditions on $u(0)$ and $u(L)$, but we have conditions on $x(0)$ and $x(L)$ instead. Second, the constants $T$, $K$, and $\sigma$ are given independently for each family of trajectories corresponding to a choice of $v_0$, $v_1$, $D_S$, and $D_U$, whereas we are looking for a constant common for all geodesics. Third, the theorem states that there *exists* $u_0$ in $D_S \cap B(v_0, \rho)$ and

$u_1$ in $D_U \cap B(v_1, \rho)$ such that the solution verifying $u^\dagger(0) = u_0$ and $u^\dagger(L) = u_1$ enjoys the exponential bound property. In contrast, we need that for *any* $u_0$ in $D_S \cap B(v_0, \rho)$ and $u_1$ in $D_U \cap B(v_1, \rho)$ such that there exists a solution verifying $u^\dagger(0) = v_0$ and $u^\dagger(T) = v_1$, the bound holds. All this makes the case of turnpike geodesics different. Now, we propose and discuss the following conjecture.

**Conjecture 1.** *Let $F$ denote a left-invariant reversible Finsler operator on the Lie group $X$. If there exists $\bar{u}$ in $\mathfrak{X}$ such that $\bar{u}$ and $-\bar{u}$ are the only saddle points on the unit sphere for the Lie algebra dynamics $D$ then the left-invariant vector field $V_x = \tilde{L}_x \bar{u}$ is an exponential geodesic turnpike for the Finsler distance associated with $F$ on $X$.*

We now provide a sketch of the proof. Critical elements are still under development and will be addressed in future publications.

Suppose $\bar{u}$ and $-\bar{u}$ are the only saddle points as defined in Definition 2, the reversibility of geodesics implies that if $\gamma^\dagger(t)$ is a geodesic of length $L$ connecting $x_0$ to $x_1$ then $\gamma^\dagger(L-t)$ is a geodesic of length $L$ connecting $x_1$ to $x_0$. By the chain rule, if $\gamma^\dagger(t)$ verifies the exponential bound with $-\bar{u}$, $\gamma^\dagger(L-t)$ verifies the exponential bound with $\bar{u}$. Note that the mapping $u \mapsto F(e, u)$ is a norm on $\mathfrak{X}$, and we can use Theorem 2 with this norm. We have the existence of constants $T$, $K$ and $\sigma$ for any choice of $v_0$ in $S$ the stable manifold of $\bar{u}$ and $v_1$ in $U$ the unstable manifold of $\bar{u}$. If we can choose the transverse discs $D_S(v_0)$ for each $v_0$ in $S$ such that the family $(D_S(v_0))_{v_0 \in S}$ forms a cover of $\mathbb{S}_F(1)$ and similarly choose the $D_U$ such that $(D_U(v_1))_{v_1 \in U}$ is also cover of $\mathbb{S}_F(1)$, then each geodesic will have their endpoints in a pair $(D_S(v_0), D_U(v_1))$. Under sufficient regularity conditions for the constants $T$, $K$, and $\sigma$, since $S$ and $U$ are included in $\mathbb{S}_F(1)$, which is compact, we can take $T^*, K^*$ as the supremum of $T, K$ and $\sigma^*$ as the infimum of $\sigma$ over the set $S \times U$.

Proving (1) the existence of such covers and (2) the regularity of the constants is challenging due to the difficulty of analytically characterizing the stable and unstable manifolds, and it is left for future work.

Suppose we have such covers. We have $T^*$, $K^*$, and $L^*$ such that for all $x_0$ and $x_1$, the parametrization by arclength $\gamma^\dagger : [0, d(x_0, x_1)] \to X$ of a geodesic connecting $x_0$ and $x_1$ or $x_1$ and $x_0$ we have for all $t$ in $[0, d(x_0, x_1)]$

$$F(e, \tilde{L}^{-1}_{\gamma^\dagger(t)} \dot{\gamma}^\dagger(t) - \bar{u}) \leq K^* \left( e^{-\sigma^* t} + e^{-\sigma^*(d(x_0,x_1)-t)} \right), \tag{22}$$

and we also have $F(e, \tilde{L}_{\gamma^\dagger(t)^{-1}} \dot{\gamma}^\dagger(t) - \bar{u}) = F(\gamma^\dagger(t), \dot{\gamma}^\dagger(t) - \tilde{L}_{\gamma^\dagger(t)} \bar{u})$ using the left-invariance (15) of $F$ with $h = \gamma^\dagger(t)$. Thus, the vector field $V_x = \tilde{L}_x \bar{u}$ is an exponential geodesic turnpike for $F$ on $X$.

The following section presents as a proof of concept the use of Conjecture 1, assumed to hold, to analyze the examples given in Fig. 1.

# 4 Preliminary applications of Conjecture 1

## 4.1 Geodesic turnpikes for a simple Riemannian distance

We study the existence of geodesic turnpikes for a simple left-invariant Riemannian metric structure on SE(2) proposed by Žefran in [35] and illustrated in Fig. 1(left). The detailed derivations are given in Appendix E.

Let $X = \mathrm{SE}(2)$ be the group of rigid transformation of $\mathbb{R}^2$, and $\mathfrak{X} = \mathfrak{se}(2)$ the Lie algebra of instantaneous motions. We denote by $v_x$, $v_y$ and $\omega$ the three coordinates of an element $u$ in the canonical basis of $\mathfrak{se}(2)$. With a slight abuse of notations, we write $u = [v_x, v_y, \omega]$. The left-invariant Riemannian operator used by Žefran to generate the geodesic in Fig. 1(left) is $F(e,u) = \sqrt{u^\top G u}$ with

$$G = \begin{bmatrix} \alpha & 0 & 0 \\ 0 & 1 & 0 \\ 0 & 0 & 1 \end{bmatrix}, \tag{23}$$

where $\alpha > 1$. The matrices representation of $\mathrm{ad}_u$ and $\mathrm{P}_u$ in the canonical basis of $\mathfrak{se}(2)$ are

$$\mathrm{ad}_u = \begin{bmatrix} 0 & -\omega & v_y \\ \omega & 0 & -v_x \\ 0 & 0 & 0 \end{bmatrix} \quad \text{and} \quad \mathrm{P}_u = \begin{bmatrix} 0 & 0 & v_y \\ 0 & 0 & -v_x \\ -v_y & v_x & 0 \end{bmatrix}. \tag{24}$$

Let us recall that for a Riemannian distance $G_u = G$, so

$$\mathrm{ad}_u^\top G_u u = \begin{bmatrix} v_y\omega \\ -\alpha v_x \omega \\ (\alpha-1)v_x v_y \end{bmatrix}. \tag{25}$$

An equilibrium point $\bar{u}$ satisfies $\mathrm{ad}_u^\top G_u u$. Since $\alpha - 1 \neq 0$, (25) implies that at least two components of $\bar{u}$ must be zero. Using the fact that an equilibrium point also satisfies $\bar{u}^\top G_{\bar{u}} \bar{u} = 1$ we obtain exactly six equilibrium points on $\mathbb{S}_F(1)$

$$\begin{aligned} &\bar{u}_1 = \alpha^{-1/2} e_1, \quad \bar{u}_2 = e_2, \quad \bar{u}_3 = e_3, \\ &\bar{u}_4 = -\alpha^{-1/2} e_1, \quad \bar{u}_5 = -e_2, \quad \bar{u}_6 = -e_3, \end{aligned} \tag{26}$$

where $(e_1, e_2, e_3)$ is the canonical basis of $\mathfrak{se}(2)$. We now calculate the Jacobian for these six equilibrium points to find the saddle points. Substituting (23) and (24) in the expression of $J_u$, (19), we obtain

$$J_u = \begin{bmatrix} 0 & \omega/\alpha & v_y/\alpha \\ -\alpha\omega & 0 & -\alpha v_x \\ (\alpha-1)v_y & (\alpha-1)v_x & 0 \end{bmatrix}. \tag{27}$$

Observe that the basis $(e_1, e_2, e_3)$ is orthogonal for the inner product induced by $G$ because $G$ is diagonal. Thus, the tangent plane to $\mathbb{S}_F(1)$ in $\bar{u}_1$, denoted by $A_1$, is spanned by $e_2$ and $e_3$; and $J_{\bar{u}_1}|_{A_1}$ is the 2 by 2 sub-matrix of $J_u$ composed

of the two last columns and two last rows of (27). The same reasoning holds for the tangent plane $A_2$ in $\bar{u}_2$ and the tangent plane $A_3$ in $\bar{u}_3$. We obtain

$$J_{\bar{u}_1}|_{A_1} = \begin{bmatrix} 0 & -\alpha^{1/2} \\ \alpha^{-1/2}(\alpha-1) & 0 \end{bmatrix}, \tag{28}$$
$$J_{\bar{u}_2}|_{A_2} = \begin{bmatrix} 0 & 1/\alpha \\ (\alpha-1) & 0 \end{bmatrix}, \quad J_{\bar{u}_3}|_{A_3} = \begin{bmatrix} 0 & 1/\alpha \\ -\alpha & 0 \end{bmatrix}.$$

The Jacobians for $\bar{u}_4$, $\bar{u}_5$ and $\bar{u}_6$ are the opposite of the ones for $\bar{u}_1$, $\bar{u}_2$ and $\bar{u}_3$. The eigenvalues of those Jacobians are given by the roots of their characteristic polynomial (see Appendix E for details). $J_{\bar{u}_1}|_{A_1}$ and $J_{\bar{u}_3}|_{A_3}$ have purely imaginary eigenvalues because $\alpha - 1 > 0$ and $\bar{u}_1$, $\bar{u}_3$, $\bar{u}_4$ and $\bar{u}_6$ are not saddle points. On the other hand, $J_{\bar{u}_2}|_{A_2}$ has eigenvalues $\pm\sqrt{(\alpha-1)/\alpha}$, with one positive and one negative, making $\bar{u}_2 = e_2$ and $\bar{u}_5 = -e_2$ the only saddle points. These vectors are precisely the translations along the $y$ axis of the local frame, i.e., parallel to the short side of the rectangle. Conjecture 1 implies that the left-invariant vector field $V_x = \tilde{L}_x e_2$ is an exponential geodesic turnpike. This matches the turnpike behavior observed in Fig. 3 (left), suggesting the potential validity of the conjecture.

This section has demonstrated a prototypical strategy for analytically identifying the saddle points of the geodesic dynamics. In the following subsection, we present a numerical strategy for identifying the saddle points for more general distances and a procedure for using them in the computation of geodesics.

### 4.2 Geodesic turnpike for the minimum swept-volume distance

We propose a numerical procedure to accelerate the geodesic computation associated with $F$. First, an offline algorithm identifies the saddle points of the Lie algebra dynamics. Assuming Conjecture 1 holds, these points are geodesic turnpikes. Second, we propose an initialization strategy using the candidate geodesic turnpikes in a geodesic solver that significantly accelerates its convergence. It is important to note that the first part of the computation is done only once for a given Finsler operator $F$ and not for every geodesic computation. Thus, identifying candidate geodesic turnpikes benefits motion planners such as RRT and its variants [21]. We assume that $F$ is a left-invariant Finsler operator known in closed form as a function of $u$, an element of the Lie algebra. This is the case for the minimum swept-volume distance for a moving rod [23]. Note that Figures 1, 2 and 3 illustrate geodesics computed with this operator. We use this example throughout the section and use the geodesic turnpikes to compute the same geodesics significantly faster.

**Saddle points identification.** We implement the symbolic expression of $F(e, u)$, $\mathrm{ad_u}$ and $\mathrm{P_u}$ in the symbolic automatic differentiation framework CasADi [1]. We use automatic differentiation to compute symbolic expressions for the Hessian of $F$ and, in turn, for $G_u$, $D(u)$, and $J_u$. We use the non-linear root finding engine implemented in CasADi with multiple initializations to identify the roots

of the system (18), i.e., the equilibrium points $\bar{u}_i$, and thus the numerical matrices $J_i = J_{\bar{u}_i}$. We use a sequence of matrix factorization routines detailed in Appendix F to compute the spectrum of the Jacobian restricted to the tangent plane of $\mathbb{S}_F(1)$ in $\bar{u}_i$. We only keep the $\bar{u}_i$ that are saddle points.

When applied to the minimum swept-volume distance of a moving rod, this algorithm yields exactly two turnpikes: the instantaneous translation parallel to the long side of the rod in both directions. This is consistent with the turnpike behavior observed in Fig. 1(right), hinting again at the potential validity of Conjecture 1.

**Initialization of the geodesic solver.** The geodesics in [23] are computed using a discretized version of the energy problem (16) with optimization variables $u_j$ with $j = 0..N$. To leverage the identified turnpike, we adopt a two-stage approach. First, for each saddle point $\bar{u}_i$, we initialize $u_j = \bar{u}_i$ for all $j = 0..N$, and we solve the minimization problem with $u_j$ fixed for $j = 1..N-1$ and only $u_0$ and $u_N$ as optimization variables. Second, we keep the saddle point $\bar{u}_i$ with the lowest cost error and solve the associated minimization problem a second time with all $u_j$ as optimization variables.

On an Intel(R) Core(TM) i7-8750H CPU, averaging over 100 cases, the first optimization problem takes $13 \pm 2$ ms to converge for each turnpike, and the second optimization problem takes around $110 \pm 14$ ms. In comparison, the standard optimization used in [23] takes 1.5 s to converge.

Overall, geodesic turnpike initialization improves the computation time of geodesic computation by an order of magnitude over the standard geodesic solver used in [23].

## 5 Conclusion

This paper has established a theoretical framework for exploring geodesic turnpike properties in metric structures on configuration spaces. We have introduced the concept of *exponential geodesic turnpikes* and proposed a conjecture providing a sufficient condition for a left-invariant Finsler operator to exhibit the geodesic turnpike property. The examples in Section 4 support the conjecture. Additionally, using a geodesic turnpike as an initialization for the geodesic solver of the swept-volume distance [23] offers significant computational acceleration. Future work will aim to complete the proof of Conjecture 1. Further research will also include an in-depth study of partially invariant distances and a deeper exploration of the implications of the turnpike property on various robotics applications.

**Acknowledgments.** This work was funded in part by the French government under management of Agence Nationale de la Recherche as part of the "Investissements d'avenir" program, reference ANR-19-P3IA-0001 (PRAIRIE 3IA Institute). JP was supported in part by the Louis Vuitton/ENS-PSL chair in artificial intelligence and a Global Distinguished Professorship at the Courant Institute of Mathematical Sciences and the Center for Data Science at New York University.

## References


1. Andersson, J.A.E., Gillis, J., Horn, G., Rawlings, J.B., Diehl, M.: Casadi: a software framework for nonlinear optimization and optimal control. Mathematical Programming Computation **11**(1), 1–36 (2018). https://doi.org/10.1007/s12532-018-0139-4
2. Arnol'd, V.I.: Mathematical methods of classical mechanics. Graduate Texts in Mathematics, Springer, New York, NY, 2 edn. (1989). https://doi.org/10.1007/978-1-4757-1693-1
3. Berger, M.: Geometry I. Universitext, Springer Berlin Heidelberg (2009)
4. Bucataru, I., Miron, R.: Finsler-Lagrange Geometry: Applications to Dynamical Systems. Editura Academiei Române (2007)
5. Celledoni, E., Marthinsen, H., Owren, B.: An introduction to lie group integrators – basics, new developments and applications. Journal of Computational Physics **257**, 1040–1061 (2014). https://doi.org/10.1016/j.jcp.2012.12.031, physics-compatible numerical methods
6. Chirikjian, G.S.: Stochastic Models, Information Theory and Lie Groups Volume 2, Analytic Mehods and Modern Applications. Birkhäuser Boston (2012). https://doi.org/10.1007/978-0-8176-4944-9
7. Chirikjian, G.S.: Partial bi-invariance of $SE(3)$ metrics. Journal of Computing and Information Science in Engineering **15**(1) (2015). https://doi.org/10.1115/1.4028941
8. Faulwasser, T., Grüne, L.: Chapter 11 - turnpike properties in optimal control: An overview of discrete-time and continuous-time results. In: Trélat, E., Zuazua, E. (eds.) Numerical Control: Part A, Handbook of Numerical Analysis, vol. 23, pp. 367–400. Elsevier (2022). https://doi.org/10.1016/bs.hna.2021.12.011
9. Featherstone, R.: Rigid body dynamics algorithms. Springer, New York (2008)
10. Frazzoli, E., Dahleh, M.A., Feron, E.: Maneuver-based motion planning for nonlinear systems with symmetries. IEEE Transactions on Robotics **21**(6), 1077–1091 (2005). https://doi.org/10.1109/TRO.2005.852260
11. Geshkovski, B., Zuazua, E.: Turnpike in optimal control of pdes, resnets, and beyond. Acta Numerica **31**, 135–263 (2022). https://doi.org/10.1017/S0962492922000046
12. Jallet, W., Bambade, A., Mansard, N., Carpentier, J.: Constrained differential dynamic programming: A primal-dual augmented lagrangian approach. In: IEEE/RSJ International Conference on Intelligent Robots and Systems (IROS). pp. 13371–13378 (2022). https://doi.org/10.1109/IROS47612.2022.9981586
13. Jaquier, N., Asfour, T.: Riemannian geometry as a unifying theory for robot motion learning and control. In: Billard, A., Asfour, T., Khatib, O. (eds.) Robotics Research. pp. 395–403. Springer Nature Switzerland, Cham (2023)
14. Jaquier, N., Rozo, L., Asfour, T.: Unraveling the single tangent space fallacy: An analysis and clarification for applying riemannian geometry in robot learning. ArXiv **abs/2310.07902** (2023), https://api.semanticscholar.org/CorpusID:263908813
15. Kierzenka, J., Shampine, L.F.: A bvp solver based on residual control and the maltab pse. ACM Transaction on Mathematical Software **27**(3), 299–316 (2001). https://doi.org/10.1145/502800.502801
16. Kjer, V.R.: Lie group integrators for cotangent bundles of lie groups and their application to systems of dipolar soft spheres. Oslo, Norway (2022), https://ntnuopen.ntnu.no/ntnu-xmlui/handle/11250/2450817, under supervision of Brynjulf, Owren, IMF

17. Klein, H., Jaquier, N., Meixner, A., Asfour, T.: A riemannian take on human motion analysis and retargeting. In: IEEE/RSJ International Conference on Intelligent Robots and Systems (IROS). pp. 5210–5217. IEEE (2022). https://doi.org/10.1109/IROS47612.2022.9982127
18. Kuehn, C.: Multiple Time Scale Dynamics. Applied Mathematical Sciences, Springer International Publishing (2016)
19. Kuffner, J.J.: Effective sampling and distance metrics for 3d rigid body path planning. IEEE International Conference on Robotics and Automation (ICRA) **2004**(4), 3993–3998 (2004). https://doi.org/10.1109/robot.2004.1308895
20. Latifi, D., Razavi, A.: Bi-invariant finsler metrics on lie groups. Australian Journal of Basic and Applied Science **5**(12), 507–511 (2011)
21. LaValle, S.M.: Planning Algorithms. Cambridge University Press (2006)
22. McKenzie, L.W.: Turnpike theory. Econometrica **44**(5), 841–865 (1976)
23. de Mont-Marin, Y., Ponce, J., Laumond, J.P.: A minimum swept-volume metric structure for configuration space. In: IEEE International Conference on Robotics and Automation (ICRA). pp. 3686–3692 (2023). https://doi.org/10.1109/ICRA48891.2023.10161367
24. Onishchik, A.L., Vinberg, E.B.: Lie Groups and Algebraic Groups. Springer Berlin Heidelberg (1990). https://doi.org/10.1007/978-3-642-74334-4
25. Paiola, L., Grioli, G., Bicchi, A.: On the evaluation of collision probability along a path (2023)
26. Palmieri, L., Arras, K.: Distance metric learning for rrt-based motion planning with constant-time inference. IEEE International Conference on Robotics and Automation (ICRA) **2015** (2015). https://doi.org/10.1109/ICRA.2015.7139246
27. Potra, F.A., Wright, S.J.: Interior-point methods. Journal of Computational and Applied Mathematics **124**(1), 281–302 (2000). https://doi.org/10.1016/S0377-0427(00)00433-7, numerical Analysis 2000. Vol. IV: Optimization and Nonlinear Equations
28. Ratliff, N.D., Van Wyk, K., Xie, M., Li, A., Rana, M.A.: Generalized nonlinear and finsler geometry for robotics. In: IEEE International Conference on Robotics and Automation (ICRA). pp. 10206–10212 (2021). https://doi.org/10.1109/ICRA48506.2021.9561543
29. Ratliff, N.D., Zucker, M., Bagnell, J.A., Srinivasa, S.S.: Chomp: Gradient optimization techniques for efficient motion planning. In: IEEE International Conference on Robotics and Automation (ICRA). IEEE (2009). https://doi.org/10.1109/robot.2009.5152817
30. Sakamoto, N., Zuazua, E.: The turnpike property in nonlinear optimal control–a geometric approach. Automatica **134**, 109939 (2021). https://doi.org/10.1016/j.automatica.2021.109939
31. Solà, J., Deray, J., Atchuthan, D.: A micro lie theory for state estimation in robotics. ArXiv **abs/1812.01537** (2018), https://dblp.org/rec/journals/corr/abs-1812-01537.bib
32. Trélat, E., Zuazua, E.: The turnpike property in finite-dimensional nonlinear optimal control. Journal of Differential Equations **258**(1), 81–114 (2015). https://doi.org/10.1016/j.jde.2014.09.005
33. Van Wyk, K., Xie, M., Li, A., Rana, M.A., Babich, B., Peele, B., Wan, Q., Akinola, I., Sundaralingam, B., Fox, D., Boots, B., Ratliff, N.D.: Geometric fabrics: Generalizing classical mechanics to capture the physics of behavior. IEEE Robotics and Automation Letters **7**(2), 3202–3209 (2022). https://doi.org/10.1109/LRA.2022.3143311

34. Žefran, M., Kumar, V., Croke, C.B.: Choice of riemannian metrics for rigid body kinematics. International Design Engineering Technical Conferences and Computers and Information in Engineering Conference (IDETC/CIE) **2B-1996**(3), 1–23 (1996). https://doi.org/10.1115/96-DETC/MECH-1148
35. Žefran, M., Kumar, V., Croke, C.B.: On the generation of smooth three-dimensional rigid body motions. IEEE Transactions on Robotics and Automation **14**(4), 576–589 (1998). https://doi.org/10.1109/70.704225
36. Zhang, L., Kim, Y.J., Manocha, D.: C-DIST. In: ACM symposium on Solid and physical modeling (SPM). ACM Press (2007). https://doi.org/10.1145/1236246.1236270

# Appendix

## A Proof of Finsler operator properties

We will prove five properties of the Finslerian operator $F$ and the associated bilinear form $g$ as defined in (10). The ones mentioned in Section 2 are properties 1, 2, 5, and the remaining ones are useful for the proof of Proposition 2 in C.

*Property 1.* For any $x$ in $X$ and $v$ in $T_xX$ we have $F^2(x,v) = g(x,v)(v,v)$.

*Proof.* Using the definition

$$\begin{aligned} g(x,v)(v,v) &= \frac{1}{2}\,\frac{\partial^2}{\partial s \partial t} F^2(x, v+sv+tv)\Big|_{s=0,t=0} \\ &= \frac{\partial^2}{\partial s \partial t}\frac{1}{2}(1+s+t)^2\Big|_{s=0,t=0} F^2(x,v) \\ &= F^2(x,v). \end{aligned} \tag{29}$$

*Property 2.* For any $x$ in $X$, $v$ in $T_xX$ and $\lambda > 0$ we have

$$g(x, \lambda v) = g(x,v). \tag{30}$$

*Proof.* For any $a$ and $b$ in $T_xX$ we have

$$\begin{aligned} g(x,\lambda v)(a,b) &= \frac{1}{2}\lim_{s\to 0^+, t\to 0^+} \frac{F^2(x, \lambda v + sa + tb)}{st} \\ &= \frac{1}{2}\lim_{s\to 0^+, t\to 0^+} \frac{\lambda^2 F^2(x, v + (s/\lambda)a + (t/\lambda)b)}{\lambda^2 (s/\lambda)(t/\lambda)} \\ &= \frac{1}{2}\lim_{s'\to 0^+, t'\to 0^+} \frac{F^2(x, v + s'a + t'b)}{s't'} \\ &= g(x,v)(a,b), \end{aligned} \tag{31}$$

where we use the changes of variables $s' = s/\lambda$ and $t' = t/\lambda$.

*Property 3.* We denote by $C$ the tri-linear symmetric form called the Cartan tensor [4] defined for any $a, b, c$ in $T_xX$ as

$$C(x,v)(a,b,c) = \frac{1}{2}\,\frac{\partial^3}{\partial s \partial t \partial u} F^2(x, v+sa+tb+uc)\Big|_{s=0,t=0,u=0}. \tag{32}$$

For any $x$ in $X$ and $v, a, b$ in $T_xX$ we have

$$C(x,v)(v,a,b) = 0. \tag{33}$$

*Proof.*

$$\begin{aligned} C(x,v)(v,a,b) &= \frac{1}{2}\,\frac{\partial^3}{\partial s\partial t\partial u}F^2(x,v+sv+ta+ub)\Big|_{s=0,t=0,u=0} \\ &= \frac{\partial}{\partial s}\left[\frac{1}{2}\,\frac{\partial^2}{\partial t\partial u}F^2(x,(1+s)v+ta+ub)\Big|_{t=0,u=0}\right]_{s=0} \\ &= \frac{\partial}{\partial s}g(x,(1+s)v)(a,b)\Big|_{s=0} \\ &= \frac{\partial}{\partial s}g(x,v)(a,b)\Big|_{s=0} \qquad\qquad = 0, \end{aligned}$$

where we used the property 2 between the second to last and last equality.

*Property 4.* For any $x$ in $X$ and $v,a,b$ in $T_xX$ we have

$$\frac{\partial}{\partial s}g(x,v+sa)(v,b)\Big|_{s=0} = 0, \tag{34}$$

*Proof.* We have $\frac{\partial}{\partial s}g(x,v+sa)(v,b)\big|_{s=0} = C(x,v)(v,a,b)$ hence the result using property 3.

*Property 5.* For any $x$ in $X$ and $v,w$ in $T_xX$ we have

$$\frac{1}{2}\,\frac{\partial}{\partial s}F^2(x,v+sw)\Big|_{s=0} = g(x,v)(v,w). \tag{35}$$

*Proof.* Using the property 1, we have

$$\begin{aligned} F^2(x,v+sw) &= g(x,v+sw)(v+sw,v+sw) \\ &= g(x,v+sw)(v,v)+2sg(x,v+sw)(v,w)+s^2g(x,v+sw)(w,w). \end{aligned} \tag{36}$$

Taking the derivative with respect to $s$, we have

$$\begin{aligned} \frac{\partial}{\partial s}F^2(x,v+sw) =& \frac{\partial}{\partial s}g(x,v+sw)(v,v) && \text{(37a)}\\ &+2g(x,v+sw)(v,w) && \text{(37b)}\\ &+2s\frac{\partial}{\partial s}g(x,v+sw)(v,w) && \text{(37c)}\\ &+2sg(x,v+sw)(w,w) && \text{(37d)}\\ &+s^2\frac{\partial}{\partial s}g(x,v+sw)(w,w). && \text{(37e)} \end{aligned}$$

When $s=0$ (37c), (37d), (37e) vanishes and using property 4 the term (37a) is equal to 0. Only (37b) is non zero, and we obtain

$$\frac{\partial}{\partial s}F^2(x,v+sw)\Big|_{s=0} = g(x,v)(v,w) \tag{38}$$

Hence, the final result.

In the rest of the appendices, given a map $f : \mathfrak{X} \times Y \to Z$ with $Y$ a manifold and $Z$ a vector space, for any $u$ in $\mathfrak{X}$, $y$ in $Y$ we denote by $\frac{\partial}{\partial u} f\big|_{u,y}$ the linear map from $\mathfrak{X}$ onto $Z$ defined for any $v$ in $\mathfrak{X}$ as

$$\frac{\partial}{\partial u} f\bigg|_{u,y} v = \frac{\partial}{\partial s} f(u + sv, y)\bigg|_{s=0}. \tag{39}$$

## B Proof of Proposition 1

***Proposition.*** *For any $\epsilon > 0$, there exists $\tau > 0$ such that for any curve $\gamma^\dagger$ parametrized by arclength and representing a geodesic, if $I_\epsilon$ denote the set of $t$ such that $F\left(\gamma^\dagger(t), \dot\gamma^\dagger(t) - V_{\gamma^\dagger(t)}\right) \geq \epsilon$ we have*

$$L\left(\gamma^\dagger|_{I_\epsilon}\right) \leq \tau. \tag{14}$$

*Proof.* Using the notation of Definition 1, let $\gamma^\dagger$ a parametric curve representing a geodesic joining $x_0$ to $x_1$ with constant velocity and of length, $L = d(x_0, x_1)$ verifying Definition 1. For any $\epsilon > 0$ we chose $\tau = (2/\sigma)\ln(2K/\epsilon)$, which is independent of the length $L$ and we verify:

- for any $t > \tau/2$ we have $e^{-\sigma t} < e^{-\sigma\frac{\tau}{2}} = e^{-\ln(2K/\epsilon)} = \epsilon/(2K)$,
- for any $t < L - \tau/2$ we have $e^{-\sigma(L-t)} < e^{-\sigma(L-(L-\frac{\tau}{2})} = e^{-\sigma\frac{\tau}{2}} = \epsilon/(2K)$.

Summing up, we have

$$\begin{aligned} &\left(\gamma^\dagger(t), \dot\gamma^\dagger(t) - V_{\gamma^\dagger(t)}\right) \leq K\left(e^{-\sigma t} + e^{-\sigma(L-t)}\right) \leq \epsilon, \\ &\forall t \in [\tau/2, L] \cap [0, L - \tau/2]. \end{aligned} \tag{40}$$

Thus, if $I_\epsilon$ denote the interval of $t$ such that $F\left(\gamma^\dagger(t), \dot\gamma^\dagger(t) - V_{\gamma^\dagger(t)}\right) > \epsilon$ we have

$$I_\epsilon \subset [0, L] \setminus ([\tau/2, L] \cap [0, L - \tau/2]) \subset [0, \tau/2] \cup [L - \tau/2, L], \tag{41}$$

and $\mu(I_\epsilon) \leq \mu([0, \tau/2]) + \mu([0, \tau/2]) = \tau$, hence the result.

## C Proof of Proposition 2

***Proposition.*** *If $F$ is a left-invariant Finsler distance on the Lie group $X$, then the geodesic equation associated with* (16) *can be written in some basis of the Lie algebra $\mathfrak{X}$ as:*

$$\begin{aligned} \dot\gamma(t) &= \widetilde{L}_{\gamma(t)} u(t), \\ \dot u(t) &= G_{u(t)}^{-1}\, \mathrm{ad}_{u(t)}^\top\, G_{u(t)} u(t), \end{aligned} \tag{17}$$

*where $G_u$ denotes the matrix representation of $g(e, u)$ in the chosen basis, $\mathrm{ad}_u$ denotes the matrix representation in that basis of the Lie algebra adjoint operator $\mathrm{ad}_u$, which captures the action of $u$ on the rest of the algebra via the Lie bracket on $\mathfrak{X}$. The solutions represent local geodesics and do not depend on the choice of basis.*

*Proof.* The Hamiltonian of the variational problem (16) reads

$$H(x,p,u) =< p, \tilde{L}_x u >_x - C(u), \tag{42}$$

where and $u \in \mathfrak{X}$ and $(x,p) \in T^*X$ the co-tangent of $X$, i.e., $x \in X$ and $p$ is a linear form on $T_xX$. $< p, v >_x$ is the dual bracket that takes a covector and a vector and returns the scalar obtained by applying the covector on the vector on the tangent space in $x$. The cotangent bundle $T^*X$ of a Lie group $X$ is a trivial bundle[5], and the Hamiltonian equations for all $t$ are:

$$\dot{x}(t) = \left.\frac{\partial H}{\partial p}\right|_{x(t),p(t),u(t)} = \tilde{L}_{x(t)} u(t), \tag{43a}$$

$$\dot{p}(t) = -\left.\frac{\partial H}{\partial x}\right|_{x(t),p(t),u(t)} = -\left.\frac{\partial < p, \tilde{L}_x u >_x}{\partial x}\right|_{x(t),p(t),u(t)}, \tag{43b}$$

$$0 = \left.\frac{\partial H}{\partial u}\right|_{x(t),p(t),u(t)} = \left.\frac{\partial < p, \tilde{L}_x u >_x}{\partial u}\right|_{x(t),p(t),u(t)} - \left.\frac{\partial C}{\partial u}\right|_{u(t)}. \tag{43c}$$

We use the left trivialization of the cotangent bundle described below to simplify the Hamiltonian equations. For $(x,p)$ in $T^*X$, we denote by $p_b = p \circ \tilde{L}_x \in \mathfrak{X}^*$ the left trivialization of the covector $p$. The cotangent bundle, $T^*X$, is equipped with a natural group structure induced by the group structure of $X$ (see [24, 16] for details) and the mapping

$$\phi : (x,p) \in T^*X \mapsto (x, p_b) \in X \ltimes \mathfrak{X}^*, \tag{44}$$

is a Lie group isomorphism where $X \ltimes \mathfrak{X}^*$ is a lie-group semi-direct product with the group law

$$(x, p_b) \circ (y, q_b) = (x \circ y, \mathrm{Ad}^*_y(p_b) + q_b), \tag{45}$$

where $\mathrm{Ad}^*_y$ is the co-adjoint representation of $y \in X$ (see [24] for details).

First, we have $< p, \tilde{L}_x u >_x =< p \circ \tilde{L}_x, u >_e =< p_b, u >_e$ and the third Hamiltonian equation (43c) is equivalent to:

$$\begin{aligned} 0 &= \left.\frac{\partial < p_b, u >_e}{\partial u}\right|_{x(t),p(t),u(t)} - \left.\frac{\partial C}{\partial u}\right|_{u(t)}, \\ p_b(t) &= \left.\frac{\partial C}{\partial u}\right|_{u(t)}. \end{aligned} \tag{46}$$

[5] its topology is the one of a Cartesian product between the base space $X$ and a fiber

Second, we denote by $\pi : (x, p_b) \in X \ltimes \mathfrak{X}^* \to p_b$ the projection, and we use the left Jacobian, as coined in [31], for $v$ in $\mathfrak{X}$ we have

$$\begin{aligned}
\frac{\partial \pi}{\partial x}(\tilde{L}_x v) &= \frac{\partial}{\partial s}\pi((x, p_b) \circ (\exp(sv), 0))\Big|_{s=0} \\
\frac{\partial p_b}{\partial x}(\tilde{L}_x v) &= \frac{\partial}{\partial s}\operatorname{Ad}^*_{\exp(sv)}(p_b) + 0\Big|_{s=0} \\
&= \frac{\partial}{\partial s}\exp(s \operatorname{ad}^*_v)\Big|_{s=0}(p_b) \\
&= \operatorname{ad}^*_v(p_b). \qquad (47)
\end{aligned}$$

We denote by $\psi$ the linear form on $\mathfrak{X}$ defined as

$$\psi = -\frac{\partial < p_b, u >_e}{\partial x} \circ \tilde{L}_x, \qquad (48)$$

for any $v \in \mathfrak{X}$ we have

$$\begin{aligned}
\psi(v) &= - < \frac{\partial p_b}{\partial x}(\tilde{L}_x v), u >_e \\
&= - < \operatorname{ad}^*_v(p_b), u >_e \\
&= - < p_b, \operatorname{ad}_v(u) >_e \\
&=< p_b, \operatorname{ad}_u(v) >_e \\
&=< \operatorname{ad}^*_u(p_b), v >_e, \qquad (49)
\end{aligned}$$

and we conclude that $\psi = \operatorname{ad}^*_u(p_b)$. Composing the second Hamiltonian equation (43b) on both side with $\tilde{L}_x$, the second Hamiltonian equation is equivalent to

$$\begin{aligned}
\dot{p_b} &= -\frac{\partial < p, \tilde{L}_x u >_x}{\partial x} \circ \tilde{L}_x \\
&= -\frac{\partial < p_b, xu >_e}{\partial x} \circ \tilde{L}_x \\
&= \operatorname{ad}^*_u(p_b). \qquad (50)
\end{aligned}$$

Third, substituting (46) in (50), the Hamiltonian equations (43a), (43b), (43c) are rewritten as

$$\dot{x}(t) = \tilde{L}_{x(t)} u(t), \qquad (51a)$$

$$\frac{\partial^2 C}{\partial^2 u}\Big|_{u(t)} \dot{u}(t) = \operatorname{ad}^*_{u(t)}\left(\frac{\partial C}{\partial u}\Big|_{u(t)}\right). \qquad (51b)$$

Note that the right and left sides are in $\mathfrak{X}^*$. Note also that the previous construction is valid for any invariant cost $C$. Now, using the definition of $g$ in (10) and the property 5, we have

$$\frac{\partial^2}{\partial^2 u} C\Big|_u (v, w) = g(e, u)(v, w), \qquad (52a)$$

$$\frac{\partial}{\partial u} C\Big|_u (v) = g(e, u)(u, v). \qquad (52b)$$

Using a basis of $\mathfrak{X}$ and its dual basis, we identify elements of $\mathfrak{X}^*$ and $\mathfrak{X}$. $G_u$ is the matrix representation in this basis of $\frac{\partial^2 C}{\partial^2 u}\Big|_{u(t)}$, and $\mathrm{ad}^\top$ is the basis representation of $\mathrm{ad}^*$. Finally, we have the geodesic equation:

$$\dot{x}(t) = \tilde{L}_{x(t)} u(t), \tag{53a}$$

$$G_{u(t)} \dot{u}(t) = \mathrm{ad}^\top_{u(t)} G_{u(t)} u(t), \tag{53b}$$

hence the result.

## D Proof of Proposition 3

***Proposition.*** *An element $\bar{u}$ in the lie algebra $\mathfrak{X}$ is an equilibrium point of the dynamics $D$ on $\mathbb{S}_F(1)$ if and only if*

$$\mathrm{ad}^\top_{\bar{u}} G_{\bar{u}} \bar{u} = 0, \quad \bar{u}^\top G_{\bar{u}} \bar{u} = 1, \tag{18}$$

*In addition, the tangent space $T_{\bar{u}}\mathbb{S}_F(1)$ tangent to $\mathbb{S}_F(1)$ in $\bar{u}$ is the set of elements $v$ in $\mathfrak{X}$ such that $v^\top G_{\bar{u}} \bar{u} = 0$ and the Jacobian of the dynamics around $\bar{u}$ is*

$$J_{\bar{u}} = G^{-1}_{\bar{u}} (\mathrm{ad}^\top_{\bar{u}} G_{\bar{u}} + \mathrm{P}_{G_{\bar{u}}\bar{u}}). \tag{19}$$

*where $\mathrm{P}_{G_{\bar{u}}}$ the unique matrix defined by*

$$\forall v \in \mathfrak{X}, \quad \mathrm{P}_{G_{\bar{u}}} v = \mathrm{ad}^\top_v G_{\bar{u}}. \tag{20}$$

We will prove the proposition through a series of simple properties. We recall the expression of the dynamics:

$$D(u) = G_u^{-1} \mathrm{ad}^\top_u G_u u. \tag{54}$$

*Property 6.* If $u : I \to \mathfrak{X}$ is a solution of $\dot{u} = D(u)$ then

$$\frac{d}{dt} C(u) = 0. \tag{55}$$

*Proof.* A solution of the dynamics $\dot{u} = D(u)$ verifies

$$u^\top G_u \dot{u} = u^\top \mathrm{ad}^\top_u G_u u = (\mathrm{ad}_u u)^\top G_u u = 0, \tag{56}$$

because the mapping $u, v \mapsto \mathrm{ad}_u v$ is antisymmetric and we have $\mathrm{ad}_u u = 0$. Now, using (35) we obtain

$$\frac{d}{dt} C(u) = \frac{\partial}{\partial u} C \Big|_u \dot{u} = g(e,u)(u, \dot{u}) = u^\top G_u \dot{u} = 0, \tag{57}$$

hence the result.

The dynamics solutions have constant cost $C$ and, in turn, constant Finsler operator $F(e,u)$. We restrict the dynamics domain to $\mathbb{S}_F(1)$, the set of all $u$ such that $F(e,u)=1$.

*Property 7.* A vector $\bar{u}$ is an equilibrium point of the dynamics $D$ defined on $\mathbb{S}_F(1)$ if:

$$\mathrm{ad}_{\bar{u}}^{\top} G_{\bar{u}}\bar{u} = 0, \quad \bar{u}^{\top} G_{\bar{u}}\bar{u} = 1, \tag{18}$$

*Proof.* First, an equilibrium point verifies $D(\bar{u})=0$. With (54) and canceling the invertible matrix $G_u$, we obtain the left part of (18). Second, using property 1, $\mathbb{S}_F(1)$ is exactly the set of $u$ such that $g(e,u)(u,u) = u^{\top}G_u u = 1$ hence the result.

*Property 8.* Let $J_u$ denote the Jacobian of the dynamics $D$ taken in $u$. If $\bar{u}$ is an equilibrium point of the dynamics, then we have

$$J_{\bar{u}} = G_{\bar{u}}^{-1}(\mathrm{ad}_{\bar{u}}^{\top} G_{\bar{u}} + \mathrm{P}_{G_{\bar{u}}\bar{u}}). \tag{19}$$

*Proof.* Taking the derivative of $D$ defined in (54), we have

$$J_u v = \left[\frac{\partial}{\partial u} G_u^{-1}\bigg|_u v\right] \mathrm{ad}_u^{\top} G_u u \tag{58a}$$

$$+ G_u^{-1}\,\mathrm{ad}_v^{\top} G_u u \tag{58b}$$

$$+ G_u^{-1}\,\mathrm{ad}_u^{\top}\left[\frac{\partial}{\partial u} G_u\bigg|_u v\right] u \tag{58c}$$

$$+ G_u^{-1}\,\mathrm{ad}_u^{\top} G_u v. \tag{58d}$$

The term (58c) is zero because $\left[\frac{\partial}{\partial u}G_u\big|_u v\right] u$ is the transpose of the matrix representation of the linear mapping
$w \in \mathfrak{X} \to \frac{\partial}{\partial s} g(e, u+sv)(u,w)\big|_{s=0}$ which is zero as stated in Property 4. Using $\mathrm{ad}_v^{\top} G_u u = \mathrm{P}_{G_u u}\, v$ with P defined in (20) and identifying $D$ we obtain

$$J_u v = \left[\frac{\partial}{\partial u} G_u^{-1}\bigg|_u v\right] G_u D(u) + G_u^{-1}(\mathrm{P}_{G_u u} + \mathrm{ad}_u^{\top} G_u)v. \tag{59}$$

Hence with $\bar{u}$ an equilibrium point, i.e., $D(\bar{u})=0$ we have

$$J_{\bar{u}} = G_{\bar{u}}^{-1}(\mathrm{ad}_{\bar{u}}^{\top} G_{\bar{u}} + \mathrm{P}_{G_{\bar{u}}\bar{u}}). \tag{60}$$

*Property 9.* The tangent space to $\mathbb{S}_F(1)$ in $u$, denoted by $T_u\mathbb{S}_F(1)$, is the vector space of element $v$ in $\mathfrak{X}$ such that $v^{\top}G_u u = 0$.

*Proof.* We have that $\mathbb{S}_F(1) = S_C(1/2)$, i.e., $\mathbb{S}_F(1)$ is a level set of $C$. Thus, for $u$ in $\mathbb{S}_F(1)$ the tangent space $T_u\mathbb{S}_F(1)$ is the set of vector $v$ in the kernel of the differential of $C$ in $u$:

$$\frac{\partial}{\partial u} C\bigg|_u v = 0,$$
$$g(e,u)(u,v) = u^{\top}G_u v = 0, \tag{61}$$

using property 4.

## E Details on Section 4.1

**Detailed derivation of the operators**
This section details the derivation of the expression of $\mathrm{ad}_u, \mathrm{P}_u, J_u, \mathrm{ad}_u^\top G_u u$ when $X = \mathrm{SE}(2)$, the group of rigid transformation of $\mathbb{R}^2$. SE(2) has a canonic matrix Lie group representation with the set of matrix $M$ written as

$$M = \begin{pmatrix} \cos(\theta) & -\sin(\theta) & x \\ \sin(\theta) & \cos(\theta) & y \\ 0 & 0 & 1 \end{pmatrix}, \tag{62}$$

with parameter $\theta, x, y$. We use parenthesis for the elements of the matrix group to distinguish them from the matrix written with brackets representing endomorphisms of the lie algebra. The identity matrix, i.e., the identity element of the group, is obtained with $\theta = 0, x = 0, y = 0$. Taking the derivative of $M$ with respect to the parameters at $0, 0, 0$, we obtain a lie algebra element $m$ written as

$$m = \begin{pmatrix} 0 & -\omega & v_x \\ \omega & 0 & v_y \\ 0 & 0 & 0 \end{pmatrix} = v_x e_1 + v_y e_2 + \omega e_3, \tag{63}$$
$$\text{with} \quad e_1 = \begin{pmatrix} 0\,0\,1 \\ 0\,0\,0 \\ 0\,0\,0 \end{pmatrix}, \quad e_2 = \begin{pmatrix} 0\,0\,0 \\ 0\,0\,1 \\ 0\,0\,0 \end{pmatrix}, \quad e_3 = \begin{pmatrix} 0 & -1 & 0 \\ 1 & 0 & 0 \\ 0 & 0 & 0 \end{pmatrix},$$

and $(e_1, e_2, e_3)$ is the canonical basis of the lie algebra. We denote by $u = [v_x, v_y, \omega]$ the column vector associated to $m$ and $u' = [v'_x, v'_y, \omega']$ the column vector associated to $m'$ another element of the lie algebra. The adjoint operator on a matrix lie group is the matrix commutator:

$$\begin{aligned}[m, m'] = mm' - m'm &= \begin{pmatrix} 0\,0 & (-\omega v'_y) - (-\omega' v_y) \\ 0\,0 & (\omega v'_x) - (\omega' v_x) \\ 0\,0 & 0 \end{pmatrix} \\ &= (-\omega v'_y + v_y \omega')e_1 + (\omega v'_x - v_x \omega')e_2 + 0e_3. \end{aligned} \tag{64}$$

Thus, the representation of the adjoint operator associated with the basis $(e_1, e_2, e_3)$ denoted by $\mathrm{ad}_u$ must verify
$\mathrm{ad}_u\, u' = [-\omega v'_y + v_y \omega', \omega v'_x - v_x \omega', 0]^\top$ and we have

$$\mathrm{ad}_u = \begin{bmatrix} 0 & -\omega & v_y \\ \omega & 0 & -v_x \\ 0 & 0 & 0 \end{bmatrix}. \tag{65}$$

We calculate

$$\mathrm{ad}_u^\top u' = \begin{bmatrix} 0 & \omega & 0 \\ -\omega & 0 & 0 \\ v_y & -v_x & 0 \end{bmatrix} \begin{bmatrix} v_x' \\ v_y' \\ \omega' \end{bmatrix} = \begin{bmatrix} v_y'\omega \\ -v_x'\omega \\ -v_y'v_x + v_x'v_y \end{bmatrix} = \begin{bmatrix} 0 & 0 & v_y' \\ 0 & 0 & -v_x' \\ -v_y' & v_x' & 0 \end{bmatrix} \begin{bmatrix} v_x \\ v_y \\ \omega \end{bmatrix} = \mathrm{P}_{u'}\, u, \tag{66}$$

and we obtain

$$\mathrm{P}_u = \begin{bmatrix} 0 & 0 & v_y \\ 0 & 0 & -v_x \\ -v_y & v_x & 0 \end{bmatrix}. \tag{67}$$

Now recall that

$$G = \begin{bmatrix} \alpha & 0 & 0 \\ 0 & 1 & 0 \\ 0 & 0 & 1 \end{bmatrix}, \tag{68}$$

and substituting the previous expressions in (18) and (19) we obtain

$$\mathrm{ad}_u^\top G_u u = \begin{bmatrix} 0 & \omega & 0 \\ -\omega & 0 & 0 \\ v_y & -v_x & 0 \end{bmatrix} \begin{bmatrix} \alpha v_x \\ v_y \\ \omega \end{bmatrix} = \begin{bmatrix} v_y\omega \\ -\alpha v_x\omega \\ (\alpha-1)v_xv_y \end{bmatrix}, \tag{69a}$$

$$u^\top G_u u = \alpha v_x^2 + v_y^2 + \omega^2 \tag{69b}$$

$$J_u = \begin{bmatrix} 0 & \omega/\alpha & 0 \\ -\alpha\omega & 0 & 0 \\ \alpha v_y & -v_x & 0 \end{bmatrix} + \begin{bmatrix} 1/\alpha & 0 & 0 \\ 0 & 1 & 0 \\ 0 & 0 & 1 \end{bmatrix} \begin{bmatrix} 0 & 0 & v_y \\ 0 & 0 & -\alpha v_x \\ -v_y & \alpha v_x & 0 \end{bmatrix} = \begin{bmatrix} 0 & \omega/\alpha & v_y/\alpha \\ -\alpha\omega & 0 & -\alpha v_x \\ (\alpha-1)v_y & (\alpha-1)v_x & 0 \end{bmatrix}. \tag{69c}$$

**Detailed derivation of the saddle points**
In this subsection, we detail how to compute the saddle points. The equation $\mathrm{ad}_u^\top G_u u = 0$ yields $v_x\omega = 0$, $v_y\omega = 0$ and $v_xv_y = 0$, and a solution $\bar{u}$ is a linear scaling of one of the vectors $e_1, e_2, e_3$. And $u^\top G_u u = 1$ yields six solutions

$$\begin{aligned} &\bar{u}_1 = \alpha^{-1/2} e_1, \quad \bar{u}_2 = e_2, \quad \bar{u}_3 = e_3, \\ &\bar{u}_4 = -\alpha^{-1/2} e_1, \quad \bar{u}_5 = -e_2, \quad \bar{u}_6 = -e_3. \end{aligned} \tag{70}$$

We have

$$\begin{aligned} &\bar{u}_1^\top G e_2 = \bar{u}_1^\top G e_3 = 0, \\ &A_1 = T_{\bar{u}_1}\mathbb{S}_F(1) = \mathrm{span}(e_2, e_3), \end{aligned} \tag{71}$$

and similar results with $\bar{u}_i, A_i$ for $i = 2..6$. Thus, we obtain

$$J_{\bar{u}_1}|_{A_1} = \begin{bmatrix} 0 & -\alpha^{1/2} \\ \alpha^{-1/2}(\alpha-1) & 0 \end{bmatrix}, \tag{72}$$
$$J_{\bar{u}_2}|_{A_2} = \begin{bmatrix} 0 & 1/\alpha \\ (\alpha-1) & 0 \end{bmatrix}, \quad J_{\bar{u}_3}|_{A_3} = \begin{bmatrix} 0 & 1/\alpha \\ -\alpha & 0 \end{bmatrix},$$

and $J_{\bar{u}_4}|_{A_4} = -J_{\bar{u}_1}|_{A_1}$, $J_{\bar{u}_5}|_{A_5} = -J_{\bar{u}_2}|_{A_2}$, $J_{\bar{u}_6}|_{A_6} = -J_{\bar{u}_3}|_{A_3}$. Now, denoting $P_i(x) = \det(J_{\bar{u}_i}|_{A_i} - x\,\mathrm{I}_2)$ the characteristic polynomial, we calculate

$$P_1(x) = x^2 + (\alpha - 1), \quad P_2(x) = x^2 - \frac{1}{\alpha}(\alpha - 1), \quad P_3(x) = x^2 + 1, \tag{73}$$

and $P_4 = P_1$, $P_5 = P_2$, $P_6 = P_3$. Only $P_2$ has real roots $\pm\sqrt{(\alpha-1)/\alpha}$ and only $\bar{u}_2, \bar{u}_5$ are saddle points.

## F Details on Section 4.2

We present the complete procedure to identify the geodesic turnpike candidate in Algorithm F.

**Algorithm 1** Saddle points computation

**Require:** $u$ ▷ A symbolic variable of dimension n
**Require:** $K$
**Require:** $A : u \to F(e,u), B : u \to \mathrm{ad}_u, P : u \to P_u$
$G \leftarrow \mathrm{hessian}(A)$ ▷ G is a symbolic expression
$C \leftarrow u^\top @ G @ u - 1$ ▷ C is a symbolic expression
$D \leftarrow B^\top @ G @ u$ ▷ D is a symbolic expression
$c \leftarrow []$
**while** $k \leq K$ **do** ▷ Multiple initialization
  $r \leftarrow \mathrm{root}([C, D], \mathrm{gauss}(0, 1, n))$ ▷ eq is a numerical value
  $M \leftarrow \mathrm{apply}(G, r)$
  $J \leftarrow M^{-1}(\mathrm{apply}(B, r)@M + \mathrm{apply}(P, M@r))$
  $A \leftarrow \mathrm{cholesky}(M)$
  $A \leftarrow A^{-\top} @ \mathrm{gramm}(A^\top @ \mathrm{complete}(r))$
  $A \leftarrow \mathrm{pinv}(A[1:])@J@A[1:]$
  $s \leftarrow \mathrm{diagonalization}(A)$
  $c \leftarrow \mathrm{appendif}(c, s, r)$
  $l \leftarrow l + 1$
**end while**
**return** $c$

where

- @ denotes the matrix multiplication,
- hessian compute the symbolic expression of an operator

- gauss$(0, 1, n)$ is a random vector of size $n$ following a Gaussian distribution with 0 mean and 1 standard deviation,
- root$([C, D], u_0)$ is a non-linear root solver for the combined expressions $C$ and $D$ in the symbolic variable $u$ and taking an initial guess $u0$,
- apply$(E, u_0)$ evaluate the symbolic expression $E$ in $u_0$,
- complete$(r)$ return an invertible square matrix of size $n$ with the first column being $r$,
- cholesky$(M)$ is the Cholesky decomposition of a symmetric positive definite matrix $M$,
- gramm$(M)$ return the matrix $Q$ of the QR-decomposition. It corresponds to the matrix where columns the basis obtained with the Gram-Schmidt procedure,
- pinv$(A[1:])$ gives the Moore-Penrose pseudo inverse of $A[1:]$ it correspond to the inverse of $A[1:]|_{\mathrm{Im}(A[1:])}$,
- diagonalization$(A)$ return the spectrum of the matrix $A$
- appendif$(c, s, r)$ is a custom function that appends $r$ to $c$ if the spectrum $s$ has only nonzero values and one with a positive real part and another one with a negative real part.

Note that $A = A^{-\top}\,\mathrm{gramm}(A^\top M)$ is a trick to compute the basis obtained with the Gram-Schmidt procedure using the inner product $u, v \to u^\top G v$ with $G = AA^\top$ instead of the canonical one. Then the last $n-1$ columns of $A$, denoted, $A[1:]$ form a basis of the tangent space to $\mathbb{S}_F(1)$ in $e$. Finally, the pseudo inverse of $A[1:]$ is the inverse change of basis and pinv$(A[1:])@J@A[1:]$ is $J|_A$ express in a basis of the tangent space.